

1 **REVISION 1**

2 **Competition between two redox states in silicate melts: an in-situ simultaneous**
3 **experiment at the Fe K-edge and Eu L₃-edge.**

4 Maria Rita Cicconi^{1§}, Daniel R. Neuville², Isabelle Tannou², François Baudelet³, Paul
5 Floury², Eleonora Paris¹, and Gabriele Giuli¹

6 1 – School of Science and Technology - Geology Division, University of Camerino. Via Gentile III da
7 Varano, I-62032 Camerino

8 2 - CNRS-Institut de Physique du Globe de Paris, 1, rue Jussieu, F- 75238 Paris

9 3 - Synchrotron SOLEIL, L'Orme des Merisiers-St. Aubin-BP 48, F-91192 Gif s/Yvette

10

11 **Running title: Eu and Fe in silicate melts**

12

13 **Keywords:** europium, iron, oxidation states, silicate melts, in-situ Dispersive XAS

14

15 *Corresponding author: Dr. Maria Rita Cicconi

16 e-mail: maria.rita.cicconi@fau.de

17 phone: +49 9131 85-27567

18

19

20 § Present Address:

21 Department Werkstoffwissenschaften

22 Lehrstuhl für Glas und Keramik

23 Universität Erlangen-Nürnberg

24 Martensstrasse 5, D-91058 Erlangen

25

26 **Competition between two redox states in silicate melts: an in-situ simultaneous**
27 **experiment at the Fe K-edge and Eu L₃-edge.**

28 Maria Rita Cicconi^{1§}, Daniel R. Neuville², Isabelle Tannou², François Baudelet³, Paul
29 Floury², Eleonora Paris¹, and Gabriele Giuli¹

30 1 – School of Science and Technology - Geology Division, University of Camerino, I

31 2 - CNRS-Institut de Physique du Globe de Paris, F

32 3 - Synchrotron SOLEIL, F

33 **ABSTRACT**

34 The understanding of redox equilibria, as well as, the knowledge of the elemental distribution
35 in magmatic melts are of fundamental importance in order to constrain the genesis of
36 magmas. In particular, the partitioning of trace elements (e.g. Eu) has demonstrated to be an
37 useful tool for estimating the redox conditions in Earth and Planetary materials. However, for
38 a more complete comprehension of Eu in silicate melts, still lacking are the information
39 regarding the effects of temperature (T), redox conditions, compositions and the possible
40 interference of other multivalent elements. Here we show new data on the oxidation states of
41 two commonly coexistent multivalent elements (Eu and Fe) in melts, acquired by “in-situ”
42 dispersive-X ray Absorption Spectroscopy experiments at high temperatures and at different
43 oxygen fugacity conditions. This work, for the first time, shows the possibility to monitor in
44 real-time the behaviour and valence variations of two elements under varying environmental
45 conditions (like T and redox state).

46 **INTRODUCTION**

47 Rare earth element (REE) patterns of igneous rocks provide useful information on the
48 conditions and processes during magma formation (e.g., Schnetzler and Philpotts 1970;
49 Henderson 1984; Blundy and Wood 2003). Among the 15 REE, europium is the only one
50 stable as divalent and many authors in the past decades have used Eu valence as a quantitative
51 oxybarometer in magmatic systems (e.g., Philpotts 1970; Drake 1975; McKay 1989;

52 Wadhwa, 2001; Karner et al. 2010). The distribution and behavior of multivalent elements
53 (Fe, Cr, V, Eu) reflects the prevailing redox conditions of their environment (Shearer et al.
54 2006), and their oxidation states will influence the mineral crystallization and the element
55 partitioning in a variety of geochemical systems. Thus, a complete understanding of transition
56 and RE elements is important for the geochemical and petrological interpretations of
57 magmatic processes and partition properties between melt and crystals in many planetary
58 materials. To do so, it is necessary to determine the ratios of oxidation states by means of a
59 quantitative knowledge of the effects of composition, T, and redox environment (fO_2).
60 In previous studies (Cicconi et al. 2009, 2012) it was experimentally demonstrated that Eu
61 behavior in silicate glasses is primarily controlled by the bulk composition and then by
62 temperature and redox conditions of the melt. In particular, Fe has been shown to affect Eu
63 oxidation states (Cicconi et al. 2012). Since Fe is the most abundant transition element, and its
64 redox state affects also the physical properties of magma, we dedicated our attention to the
65 interaction between Eu and Fe. Schreiber (1977) suggested that the higher reduction potential
66 of the Fe^{3+} - Fe^{2+} redox couple in silicate melts, in comparison with the reduction potential of
67 Eu^{3+} - Eu^{2+} , implies that Fe^{3+} could oxidize all the Eu^{2+} present. This interaction in silicate
68 glasses was also described for Fe and Ce (Schreiber et al. 1980).
69 In order to experimentally visualize the Eu kinetic reduction and therefore to understand how
70 Fe influences Eu-bearing melts, we have carried out a direct determination of Eu and Fe
71 valence states by dispersive-X-ray Absorption Spectroscopy (XAS).

72 **SAMPLES AND ANALYTICAL TECHNIQUES**

73 The sample investigated has an Fe-rich (~ 14wt%) basaltic composition (FeBas). The starting
74 material has been prepared from dried oxides and carbonates in stoichiometric proportions.
75 The mixture has been homogenized in an agate mortar and melted to obtain a glass
76 (T=1400°C), which was then finely ground and doped with 5wt% Eu_2O_3 . The resulting glass

77 was checked by optical microscope and scanning electron microscopy to ensure homogeneity
78 and the absence of crystalline phases (Cicconi et al. 2012 for details on the syntheses; Tab.1).
79 To carrying out the high-temperature (HT) X-ray Absorption Near-Edge Structure (XANES)
80 experiments, the samples were loaded as μg -powders in the 1-mm hole of the Pt-Ir10 %
81 heating wire of the microfurnace designed following the idea developed by Mysen and Frantz
82 (1992) and previously used for in situ XANES high temperature studies (Neuvville et al. 2008;
83 Cochain et al. 2009; Gonçalves Ferreira et al. 2013; see also Neuvville et al. 2014 for more
84 details). The XANES spectra have been collected simultaneously at the Eu L_3 -edge (6977 eV)
85 and at the Fe K-edge (7112 eV) at ODE beamline (SOLEIL, France). ODE is an energy
86 dispersive beamline with a bent Si(111) polychromator crystal at the focal point of which the
87 sample is placed. The beam size was 30 x 30 μm (FWHM). Due to the fixed energy–position
88 correlation in the diffracted energy band, a complete absorption spectrum was obtained from
89 measurements of the intensity distribution on a position-sensitive detector. The Si(111) bend
90 polychromator provides an energy resolution of ~ 1 eV at 7keV. Because a spectrum is
91 recorded in the order of seconds, this beamline is particularly well suited to investigate fast
92 reduction kinetics processes at HT. The closed microfurnace allows also the use of different
93 gases in order to obtain different redox environments. In these experiments, the first step was
94 to acquire the XAS spectra of the untreated sample (in air, at room temperature). Then, we
95 increased the temperature up to 1500°C and we monitored the changes in both the edges. The
96 final step was to change the gases into the furnace, passing from air to pure Ar, back to air
97 and finally to an Ar/H₂ gas mixture (to simulate a reducing environment). After calibration
98 (by converting pixel position to energy) the spectral background was removed and the signal
99 normalized at the Eu L_3 -edge using the Athena software (Ravel and Newville 2005). The Eu
100 threshold energy was taken as the first maximum of the first derivative of the spectra, whereas
101 peak positions were obtained by calculating the second derivative of the spectra. Eu data
102 analysis was carried out by following the procedure described in Cicconi et al (2012). In brief,

103 the peaks relative to Eu^{2+} and Eu^{3+} can be fitted by a combination of pseudo-Voigt (pV) and
104 arctangent (atg) functions to simulate the XANES spectra (i.e. Takahashi et al. 2005; Cicconi
105 et al. 2012). The pV and atg functions simulate the resonance peak and the absorption edge
106 step, respectively. The Fe pre-edge peak analysis was carried out following the same
107 procedure reported in Wilke et al. (2001) and Giuli et al. (2012) in order to extract
108 information on the Fe oxidation state. The main peak data analysis of the Eu portion of the
109 XANES spectrum was done in the energy range 6950-7020 eV, whereas the pre-edge peak
110 analysis of the Fe edge was done in the energy range 7090-7200 eV.

111 **RESULTS and DISCUSSION**

112 **Iron and europium redox reaction in a basaltic melt**

113 The XANES spectrum of the untreated basaltic sample (a glass collected in air and room T) is
114 reported in Figure 1a, along with its first derivative. The spectrum was normalized at the Eu
115 L_{3-} edge. When both Eu oxidation states are present, the XANES spectrum displays two well-
116 separated peaks related to both Eu^{2+} and Eu^{3+} contributions (Takahashi et al. 2005). A
117 comparison of our XANES peak positions with literature data of Eu and Fe model compounds
118 allows recognition of the presence of both elements prevalently in their trivalent states (Fig.
119 1a). The main peak data analysis of the Eu portion (6950-7020 eV) and the pre-edge peak
120 analysis of the Fe edge (7090-7200 eV) (see Fig. 1b-c) confirm the prevalence of Eu and Fe
121 oxidized species ($\text{Fe}^{3+}/\text{Fe}_{\text{tot}} = 0.96 \pm 0.05$).

122 The glass was then melted at 1500°C: the XANES data recorded show no marked differences
123 in the Eu portion and very small changes were detected in the Fe portion (Fig. 2). The
124 calculated $\text{Fe}^{3+}/\text{Fe}_{\text{tot}}$ ratio is 0.85 (± 0.05), after 245s at HT in air (inset in Fig. 2). Right after
125 the injection of pure Ar in the furnace it was possible to observe a significant reduction of Fe
126 in the melt (Fig. 2). In fact, through the first derivatives of the signals we observed a shift of
127 the Fe K-edge to lower energies (about 2.5 eV) whereas no significant differences occurred in
128 the Eu spectra (Fig. 2). Thus, just after 50 seconds in pure Ar the $\text{Fe}^{3+}/\text{Fe}_{\text{tot}}$ ratio was

129 estimated to be already 0.30 (± 0.05) demonstrating a strong Fe reduction. However, this
130 process was completely reversible as soon as Ar was removed, bringing the Fe ratio back to
131 higher values ($(\text{Fe}^{3+}/\text{Fe}_{\text{tot}} = 0.80 \pm 0.05)$). In these conditions, the complete absence of Eu^{2+} and
132 the significant presence of Fe^{2+} could be described by the redox reaction:

133 $\text{Eu}^{2+} + \text{Fe}^{3+} \Leftrightarrow \text{Eu}^{3+} + \text{Fe}^{2+}$ (Schreiber 1977). Thus, Fe^{3+} easily oxidized all the Eu^{2+} present.

134 The third step of the experiment consisted of the injection of a gas mixture of Ar/H₂ to
135 simulate a strong reducing environment. The material melted at 1500°C was re-equilibrated in
136 air (time 0 in Fig. 3) and as soon as we injected Ar/H₂ in the furnace box, Fe was completely
137 reduced, whereas Eu started to transform into its reduced form, but much slower than Fe. In
138 fact, it took more than 5 minutes for Eu to reach the almost pure divalent state (337s in Fig.
139 3). Figure 3 also shows the spectra acquired just before (time 0) and right after the injection of
140 Ar/H₂ (37s) and the reverse process: from Ar/H₂ atmosphere (337s) to air (after 34 s).

141 Interestingly it was observed that, in the reverse process (thus, passing from the reducing
142 environment Ar/H₂ to air), it took less than a minute for Eu to transform completely into its
143 oxidized form (about 34 seconds, Fig. 3). The experiment was done twice in order to ensure
144 the reliability of the fast oxidation. From each Eu spectrum the $\text{Eu}^{3+}/\text{Eu}_{\text{tot}}$ ratio was
145 determined (± 0.06 ; see Fig. 4). The time dependence of the Eu redox ratio in this basaltic
146 glass is reported in Figure 4 and its evolution with time at a given temperature can be
147 described by the expression that was used by Magnien et al. (2006) to study the evolution of
148 $\text{Fe}^{3+}/\text{Fe}_{\text{tot}}$:

149
$$(F_t - F_{\text{eq}}) = (F_0 - F_{\text{eq}}) \exp(-t/\tau), \quad (\text{Eq. 1})$$

150 where F_t is the redox ratio at time t , F_0 the initial ratio, F_{eq} the equilibrium value and τ a
151 characteristic time determined from a least-squares fit of Eq. (1) to the experimental redox
152 data. During the experiment, the $\text{Eu}^{3+}/\text{Eu}_{\text{tot}}$ ratio varied from 1.00 to 0.07 (± 0.06) with a well-
153 defined trend (black circles in Fig. 4). Remarkably, it took 34s for the $\text{Eu}^{3+}/\text{Eu}_{\text{tot}}$ ratio to return
154 to the value obtained in the oxidizing process (i.e. by removing the Ar/H₂ gas mixture; empty

155 circle in Fig. 4). On the contrary, the kinetic of the Fe reduction during these experiments was
156 extremely fast (66 s) and the spectra could not be recorded rapidly enough to show the
157 variations of the edge/pre-edge as a function of valence changes and time. Moreover it must
158 be noted that, at such reducing conditions, Fe strongly interacts with the Pt wire, and since
159 there is a complete solid solution between Pt and Fe, iron is not present in the sample
160 anymore, but it concentrates in the Pt wire, making the Fe edge undetectable after 200 s.

161 **IMPLICATIONS**

162 “In-situ” XAS studies can improve our understanding of the behavior of trace and transition
163 elements in melts/glasses, enhancing understanding of the experimental factors that influence
164 redox ratios. Oxidation-reduction equilibria involving e.g. Fe and Eu are very important in
165 studies of magmatic samples. In particular, since Eu anomalies in terrestrial and
166 extraterrestrial materials are largely used to determine the prevailing redox conditions, there is
167 need to fully understand the factors that influence Eu behavior in multicomponent systems,
168 such as bulk composition, temperature, and presence of other multivalent elements. Such
169 studies have been surprisingly rare for a geochemically important element such as Eu.
170 Our in-situ data on Eu are consistent with those obtained from the quenched glasses (Cicconi
171 et al. 2012). In fact, both in-situ and ex-situ data on Fe-bearing melts show that, in air and
172 under slightly reducing conditions, Eu is only present in its oxidized form. On the contrary,
173 some differences were observed for Fe. The fast reduction observed with in-situ XAS data
174 collection and the comparison with data obtained from the quenched glass, show a quench
175 effect that cannot be neglected in future studies.

176 This work, for the first time, shows the possibility to monitor in real-time the valence changes
177 of two elements in silicate glasses/melts, at different temperatures and/or redox environments.

178 We observed experimentally that there is strong competition between the two redox couples
179 investigated: Fe³⁺ could easily oxidize all the Eu²⁺ present, and consequently, in order to use
180 Eu as a quantitative oxybarometer, this mutual interaction must be taken into account.

181 Furthermore, it is generally believed that mutual redox interactions take place during the
182 quench process (i.e. Schreiber et al. 1980; Paul 1990), as a result of differences in the change
183 in free energy among the different multivalent elements (Russell 1989; Bingham et al. 2014).
184 Instead, in this study, we verified experimentally that electron transfer occurs also in the melt
185 state, and not just during the quench.

186 Finally, the procedures adopted for this experiment could be used to study many other redox-
187 couples, involving other transition elements, and could be of interest for a range of
188 applications other than the Geosciences, such as in the glass industry for technologically
189 relevant materials, or interactions in glasses for nuclear waste confinement (such as the redox-
190 couple Ce-Cr).

191 **Acknowledges**

192 The authors acknowledge SOLEIL for provision of synchrotron radiation facilities. This work
193 was supported by FIRB funds to G.G.

194 **References cited**

- 195 Bingham, P. A., Hannant, O. M., Reeves-McLaren, N., Stennett, M. C., and Hand, R. J.
196 (2014) Selective behaviour of dilute Fe³⁺ ions in silicate glasses. *Journal of Non-Crystalline*
197 *Solids*, 387, 47-56.
- 198 Blundy, J. and Wood, B. (2003) Partitioning of trace elements between crystals and melts.
199 *Earth and Planetary Science Letters* 210, 383-397.
- 200 Cicconi, M.R., Giuli, G., Paris, E., Ertel-Ingrisch, W., and Dingwell, D.B. (2009) Europium
201 structural role in silicate glasses: reduction kinetics at low oxygen fugacity. *Journal of*
202 *Physics: Conference Series*, 190, 012179.
- 203 Cicconi, M. R., Giuli, G., Paris, E., Ertel-Ingrisch, W., Ulmer, P., and Dingwell, D. B. (2012)
204 Europium oxidation state and local structure in silicate glasses. *American Mineralogist*, 97,
205 918-929.
- 206 Cochain, B., Neuville, D. R., De Ligny, D., Roux, J., Baudalet, F., Strukelj, E., and Richet, P.

- 207 (2009) Kinetics of iron redox reaction in silicate melts: A high temperature XANES study on
208 an alkali basalt. *Journal of Physics: Conference Series*, 190, 012182.
- 209 Drake, M.J. (1975) The oxidation state of europium as an indicator of oxygen fugacity.
210 *Geochimica et Cosmochimica Acta*, 39, 55-64.
- 211 Henderson, P. (1984). *Rare Earth Element Geochemistry*. Elsevier, Amsterdam, p. 115.
- 212 Farges, F. (2001) Crystal-chemistry of Fe in natural grandidierites: a XAFS spectroscopy
213 study at the Fe K-edge. *Physics and Chemistry of Minerals*, 28, 619-629.
- 214 Giuli, G., Alonso-Mori, R., Cicconi, M. R., Paris, E., Glatzel, P., Eeckhout, S. G., and
215 Scaillet, B. (2012) Effect of alkalis on the Fe oxidation state and local environment in
216 peralkaline rhyolitic glasses. *American Mineralogist*, 97, 468-475.
- 217 Gonçalves Ferreira, P., de Ligny, D., Lazzari, O., Jean, A., Cintora, O., and Neuville, D. R.
218 (2013) X-ray effect on the equilibrium redox state of iron-bearing earth alkali silicate glasses.
219 *Chemical Geology*, 346, 106-112.
- 220 Karner, J.M., Papike, J.J., Sutton, S.R., Burger, P.V., Shearer, C.K., Le, L., Newville, M., and
221 Choi, Y. (2010) Partitioning of Eu between augite and a highly spiked martian basalt
222 composition as a function of oxygen fugacity (IW-1 to QFM): Determination of $\text{Eu}^{2+}/\text{Eu}^{3+}$
223 ratios by XANES. *American Mineralogist*, 95, 410-413.
- 224 Magnien V., Neuville D.R., Cormier L., Roux J., Pinet O., and Richet P. (2006) Kinetics of
225 iron redox reactions: A high-temperature XANES and Raman spectroscopy study. *Journal of*
226 *Nuclear Materials*, 352, 190-195.
- 227 Magnien V, Neuville D.R., Cormier L., Roux J., Hazemann J-L., de Ligny D., Pascarelli S.,
228 Vickridge I., Pinet O., and Richet P. (2008) Kinetics and mechanisms of iron redox reactions
229 in silicate melts: The effects of temperature and alkali cations. *Geochimica et Cosmochimica*
230 *Acta*, 72, 2157-2168.
- 231 McKay, G.A. (1989) Partitioning of rare earth elements between major silicate minerals and
232 basaltic melts. In *Geochemistry and Mineralogy of Rare Earth Elements* (B.R. Lipin and G.A.

- 233 McKay, eds.) *Reviews in Mineralogy*, 21, 25-44.
- 234 Neuville D.R., Cormier L., Flank AM, de Ligny D., Roux J., and Lagarde P. (2008)
235 Environment around Al, Si and Ca in aluminate and aluminosilicate melts by X-ray
236 absorption spectroscopy at high temperature. *American Mineralogist*, 93, 228-234.
- 237 Neuville D.R., Hennet L., Florian P., and de Ligny D. (2014) In situ high temperature
238 experiment. In *Spectroscopic methods in Mineralogy and Material Sciences. Review in*
239 *Mineralogy and Geochemistry*, 78, 779-800.
- 240 Paul A. (1990) Oxidation-reduction equilibrium in glass. *Journal of Non-Crystalline Solids*,
241 123, 354-362.
- 242 Philpotts, J.A. (1970) Redox estimation from a calculation of Eu^{2+} and Eu^{3+} concentrations in
243 natural phases. *Earth and Planetary Science Letters*, 9, 257-268.
- 244 Ravel, B. and Newville, M. (2005) ATHENA, ARTEMIS, HEPHAESTUS: data analysis for
245 X-ray absorption spectroscopy using IFEFFIT. *Journal of Synchrotron Radiation*, 12, 537-
246 541.
- 247 Russel, C (1989) Redox reactions during cooling of glass melts. A theoretical consideration.
248 *Glastechnische Berichte*, 62, 199-203.
- 249 Schnetzler, C.C. and Philpotts, J.A. (1970) Partition coefficient of rare-earth elements
250 between igneous matrix material and rock-forming mineral phenocrysts. *Geochimica et*
251 *Cosmochimica Acta*, 34, 331-340.
- 252 Schreiber, H.D. (1977) Redox state of Ti, Zr, Hf, Cr and Eu in basaltic magmas: An
253 experimental study. *Proceeding Lunar Science Conference 8th*, 1785-1807.
- 254 Schreiber, H.D., Lauer, H.V., and Thanyasiri, T. (1980) The redox state of cerium in basaltic
255 magmas: an experimental study of iron-cerium interactions in silicate melts. *Geochimica et*
256 *Cosmochimica Acta*, 44, 1599-1612.
- 257 Shearer, C.K., Papike, J.J., and Karner, J.M. (2006) Pyroxene europium valence
258 oxybarometer: effects of pyroxene composition, melt composition, and crystallization

- 259 kinetics. *American Mineralogist*, 91, 1565-1573.
- 260 Takahashi, Y., Kolonin, G.R., Shironosova, G.P., Kupriyanova, I.I., Uruga, T., and Shimizu,
261 H. (2005) Determination of the EuII/EuIII ratios in minerals by X-ray absorption near-edge
262 structure and its application to hydrothermal deposits. *Mineralogical Magazine*, 69, 179-190.
- 263 Wadhwa, M. (2001) Redox state of Mars upper mantle and crust from Eu anomalies in
264 shergottite pyroxenes. *Science*, 291, 1527-1530.
- 265 Wilke, M., Farges, F., Petit P.E., Brown, and G.E., Martin, F. (2001) Oxidation state and
266 coordination of Fe in minerals: an Fe K-XANES spectroscopic study. *American Mineralogist*,
267 86, 714-730.
- 268

269 **Table 1** – Chemical composition of the Fe-basalt glass (wt%)

	wt%
SiO₂	47.20
Al₂O₃	9.74
FeO	14.10
CaO	3.85
MgO	5.36
K₂O	4.47
Na₂O	2.96
TiO₂	7.63
Eu₂O₃	4.91
tot	100.22

270

271

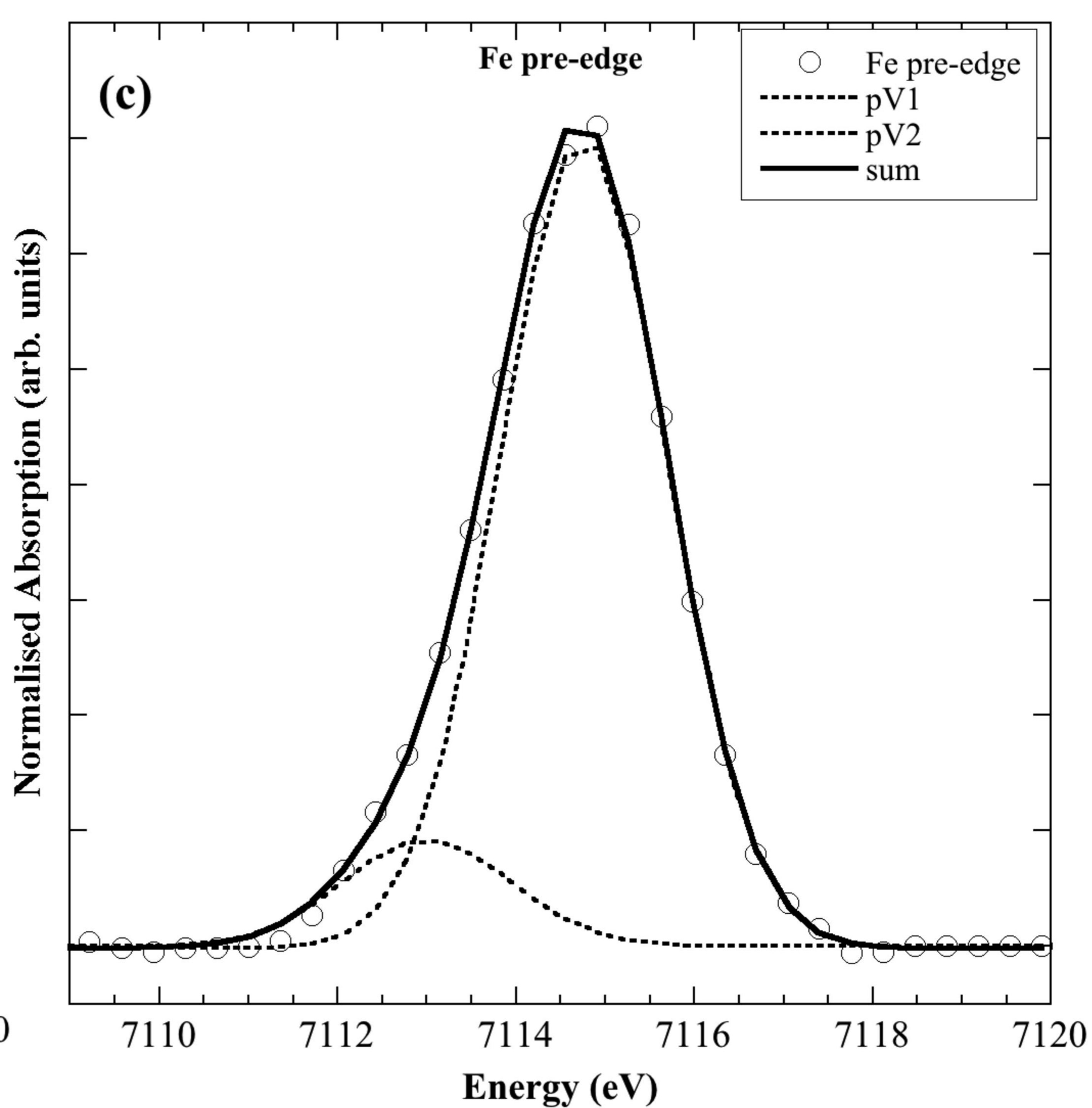
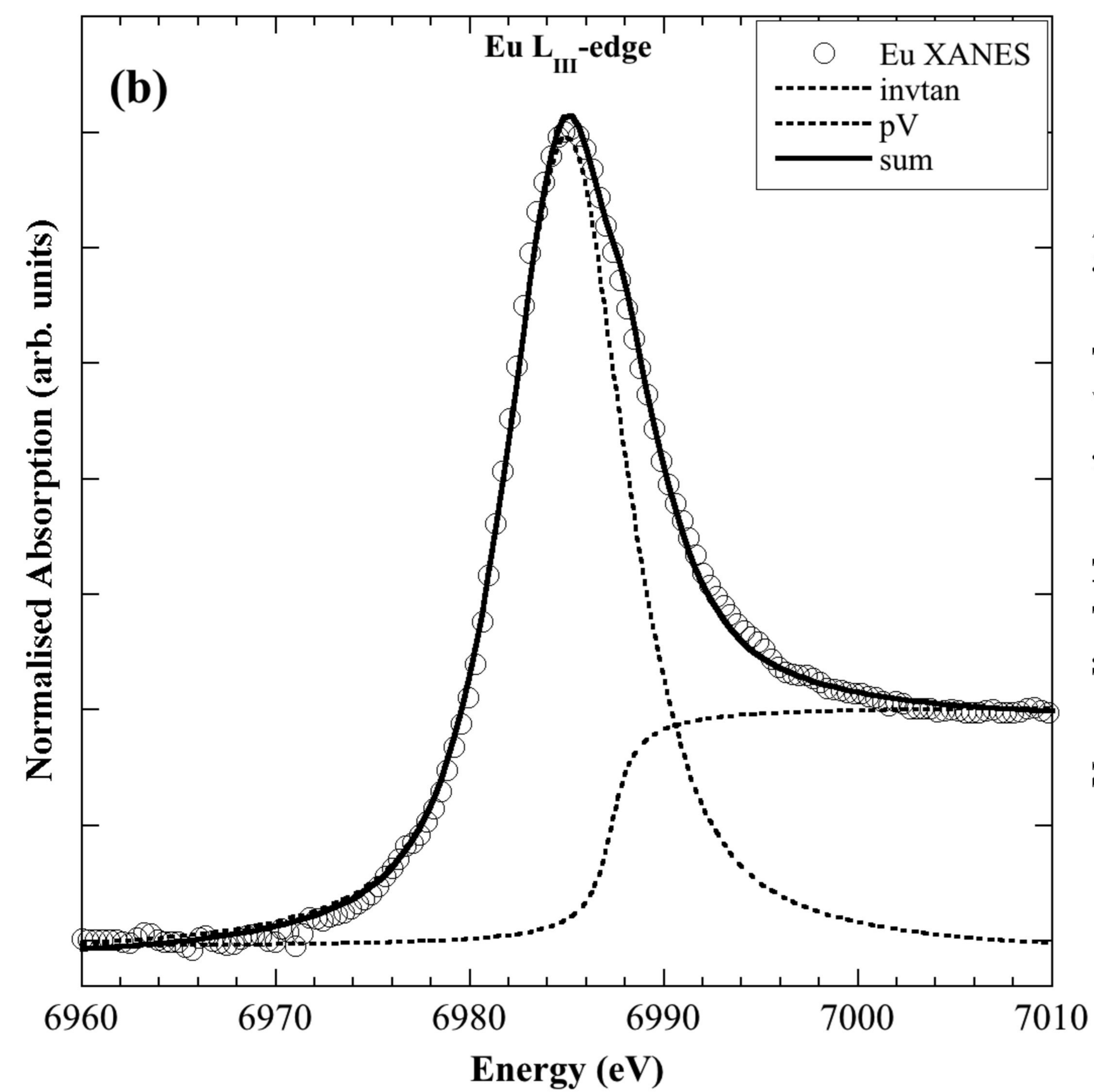
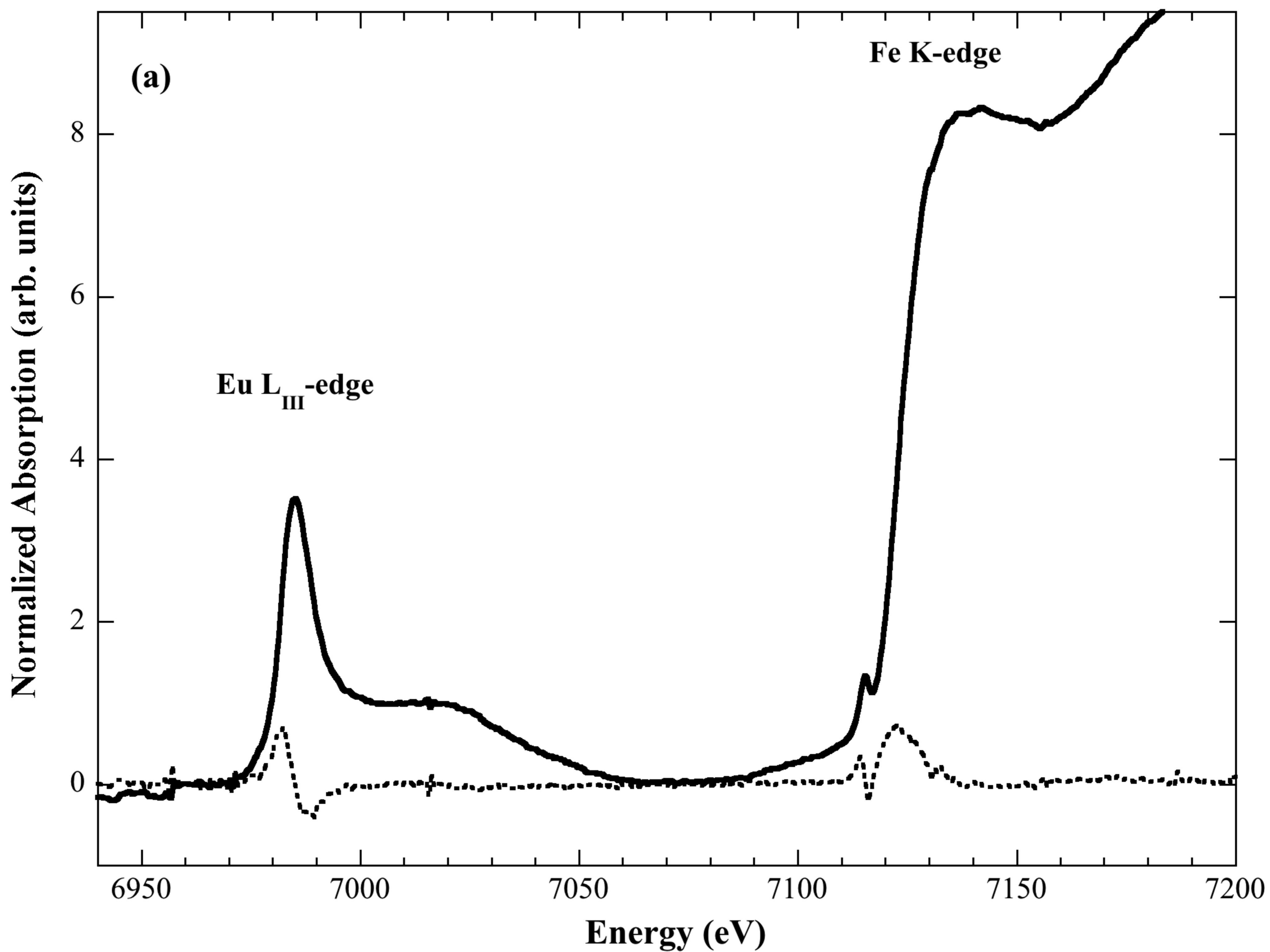
272 **Figure captions**

273 **Figure 1:** a) XANES spectrum of the untreated sample (collected in air and room T)
274 normalized at the Eu-L₃ edge, along with the first derivative. The threshold energies (taken as
275 the first maximum of the first derivative) show the dominant presence of trivalent species. b-
276 c) The main peak data analysis of the Eu portion (6950-7020 eV) (b) and the pre-edge peak
277 analysis at the Fe K-edge (7090-7200 eV) (c) are shown. Black circles indicate the
278 experimental signals, the solid lines the theoretical signals, and the dotted lines the different
279 components used for the fitting.

280 **Figure 2:** Comparison of the XANES spectra, normalized at the Eu-L₃-edge: collected for the
281 untreated sample (glass) and for the melt after 30s and 245s at 1500°C (HT-air) in air and for
282 the melt after 50s from the injection of pure Ar (HT-Ar). The inset shows the changes
283 occurring in the first derivative of the signals.

284 **Figure 3:** Comparison of the XANES spectra, normalized at the Eu-L₃-edge, collected at
285 1500°C in air (HT air) and after the injection of Ar/H₂ into the furnace box. The spectra
286 acquired just before (time 0) and right after the injection of Ar/H₂ (after 33s) and also the
287 reverse process: from Ar/H₂ atmosphere (337s) to air (after 34 s) are shown. The inset shows
288 the first derivative of the signals acquired from time 0 till 66s.

289 **Figure 4:** Time dependence of the Eu redox ratio of the basaltic sample at time 0 (air, HT)
290 and after the injection of Ar/H₂ gases (full symbols). The evolution of the europium redox
291 ratio is very fast and was calculated by using the Magnien et al (2006) expression. The empty
292 circle represents the reverse process: from Ar/H₂ atmosphere (337s) to air (time 371s).



Normalized Absorption (arb. units)

